A Markovian Model for Harvested Power from Human Motion *

Shenqiu Zhang
University of Rochester
shenqiu.zhang@rochester.edu

Alireza Seyedi
University of Central Florida
alireza.seyedi@ucf.edu

ABSTRACT

Empirical acceleration measurements are collected at 4 body locations from 20 subjects during normal daily activities. The measured acceleration is converted to the harvestable power assuming a velocity-damped resonant generator. Based on the calculated harvestable power, a simple Markovian model with two power levels and three states is developed.

Categories and Subject Descriptors

I.6 [**Simulation and Modeling**]: Probability and Statistics

General Terms

Measurement

1. INTRODUCTION

Body sensor networks [24] are envisioned to have numerous applications including health monitoring [3, 10, 17]. One of the key challenges in the design and implementation of body sensor networks is the energy supply of the nodes. This is because the nodes are expected to be inexpensive and small and, thus, have extremely limited energy storage [11]. Although a plethora of energy conserving techniques have been developed in the broader context of wireless sensor networks [7, 9, 21], the energy problem remains one of great significance for body sensor networks.

Energy harvesting is a promising approach to address the energy supply problem. To overcome the limitation of energy supply, sensors can harvest energy from the ambient sources [18] such as solar [1], wind [20], vibration [23], and thermal gradient [14]. Intrinsically the more attractive ambient sources are dynamic and random. Hence, although harvesting energy from the environment is a promising solution, it also poses a serious challenge in the design of energy usage policies and the resulting performance of the system.

*This work has been funded by the NSF grant CNS-1049691.

BODYNETS 2013, September 30-October 02, Boston, United States

DOI 10.4108/icst.bodynets.2013.253912

For a systematic approach to the design and analysis of energy harvesting sensor nodes, the stochastic nature of the energy source must be represented with a stochastic model. This can be easily seen in parallel to channel and traffic models, widely used in the analysis and design of wireless communication systems. For instance, without a proper energy model one needs to ignore the possibility that sensor nodes might harvest more energy in the future and the excess energy has to be discarded when the energy storage is full. Such an approach will clearly lead to over-designed systems. Moreover, the performance of systems involving energy harvesters cannot properly be studied without a statistical model that properly describes the harvested energy.

Some existing literature utilize historical measurements of ambient energy sources to verify their designed systems and optimize desired metrics [5] [12]. For example, [12] employs the historical records of solar insolation data through their designed system and measures the probability of battery being empty. This process is repeated many times until an optimal set of design parameters is obtained. Clearly, the design process using historical harvesting data is inefficient and does not provide a useful understanding of the characteristics of harvestable energy sources. Furthermore, it does not lend itself to any analytical approach.

In absence of such models, the existing works have had to resort to simply assuming a model for the harvested energy. For simplicity and tractability reasons, these assumed models are often Markovian [4, 13, 19, 25]. For instance, using a Markovian model, in [19] and [25] the interaction between harvesting source, load, the queueing of unprocessed events, and energy storage is studied. The probability of running out of energy and the average queueing delay on an energy-harvesting sensor node are derived. The analytical analysis is further utilized to guide a near-optimal design of sensor nodes, in terms of the capacity of energy storage and harvesting devices as well as the event queue capacity. With a similar idea, [4] models energy harvesting sensors with simpler Markov chain and studies the statistical properties of energy harvesting sensor nodes. In [13], a single-hop data transmission between energy-harvesting sensor nodes is modeled by a Markov decision process. The model uses an on-off binary decision scheme to decide transmit or drop data packets.

Despite the apparent popularity of Markovian assumption, to the best of our knowledge, there are no Markovian models

(a) Alive Heart and Activity Monitor [2]

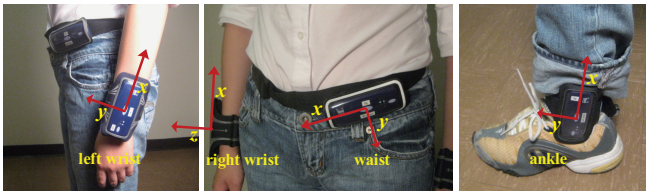

(b) Subjects wear four accelerometers

Figure 1: A subject wear four Alive Heart and Activity Monitors [2] on left wrist, right wrist, left ankle, and waist.

available that have been developed based on empirical measurements. In [22] the harvested power is measured at different body locations, and the parameters of the harvester are optimized. However, the dynamics of the harvested power are not explored. In [6] the optimal number of Markovian states is determined by minimizing the Bayesian information criterion. However, an actual model is not provided. In this paper, we develop a simple three-state Markovian model for harvested power from human motion. We develop our model based on empirical data, obtained from wearable accelerometers at four body locations.

2. HARVESTED ENERGY

2.1 Measurements

The acceleration of human motion is measured using the *Alive Heart and Activity Monitor* [2] shown in Fig. 1(a). The empirical data is collected for 20 subjects while they perform unscripted regular daily activities. The subject pool consists of 10 male and 10 female subjects, with ages ranging from 18 to 43, heights from 1.50 to 1.99 m, and weights from 45 to 95 kg. As illustrated in Fig. 1(b), subjects wore four devices on four locations on their body: left wrist, right wrist, left ankle, and waist, continuously for 2 days. They were instructed to wear the devices constantly, except during sleep and activities that may harm the device, such as taking a shower or swimming. Due to unexpected hardware malfunctions occasionally the data was not recorded. Consequently, overall 70 valid recordings were collected.

At each location the acceleration is measured in three dimensions. The alignment of the axes are shown in Fig. 1(b). The device used records samples of the acceleration at a fixed sampling rate of 75 samples per second. The samples have

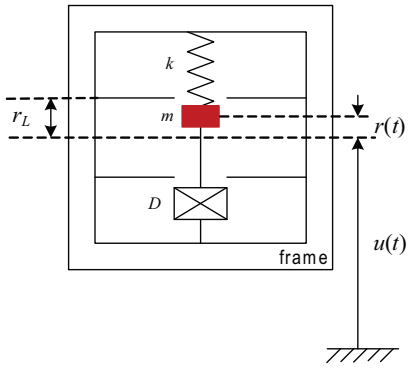

Figure 2: Model of a VDRG energy harvester.

a resolution of 8 bits and are limited to $\pm 2.7g = \pm 2.7 \times 9.81$ m/s^2 [2].

2.2 Conversion of Acceleration to Power

To remove the high-frequency noise, the measured acceleration signals are passed through a second-order Butterworth low-pass filter with cut-off frequency 35 Hz. Moreover, the gravity appears as a constant vector added to the measured acceleration signal. Thus, the denoised acceleration signal is filtered by a third-order Butterworth high-pass filter with cut-off frequency 0.4 Hz. This is the same approach used in [22].

Typical harvesting devices only harvest the energy along one particular direction [24]. Hence we consider the acceleration in each direction separately. The three orthogonal acceleration signals are converted to the harvestable energy independently. To simplify the notation, we denote the scalar acceleration, in the direction of one particular axis, after denoising and removing the gravity, by $a(t)$ in the following analysis.

We assume a velocity-damped resonant generator (VDRG) harvester [16, 22] to convert the acceleration to harvestable power. As shown in Fig. 2, in a VDRG harvester a mass is attached to a frame with a spring. The internal mass is damped by a force proportional to its velocity. The position of internal mass related to the external frame is denoted by $r(t)$, which is related to the acceleration of the external frame $a(t)$ by [16]

$$m\ddot{r}(t) = -kr(t) - D\dot{r}(t) - ma(t), \tag{1}$$

where m is the mass, k is the spring constant, and D is the proportionality factor between the damping force and the velocity of the mass. The linear relationship (1) between $a(t)$ and $r(t)$ is only valid when the internal mass moves within the limited range of frame, i.e. $|r(t)| \leq r_L$. Denoting the Laplace transforms of $a(t)$ and $r(t)$ by $A(s)$ and $R(s)$, respectively, the transfer function corresponding to (1) is

$$\frac{R(s)}{A(s)} = -\frac{1}{s^2 + \frac{D}{m}s + \frac{k}{m}},$$

which can be easily implemented to convert $a(t)$ to $r(t)$.

The damping force is proportional to the velocity of the internal mass, i.e. $f(t) = -D\dot{r}(t)$. Thus, the harvesting

power is calculated by

$$p(t) = -f(t)\dot{r}(t) = D\dot{r}^2(t).$$

2.3 Optimization of System Parameters

Clearly, the converted energy and, therefore, the statistical model depend on the parameters of the VDRG harvester, m, k and D. Thus, first we attempt to optimize these parameters. In practice, one would like to choose these parameters such that (average) harvested energy is maximized. Since different sets of optimal parameters will maximize the average harvested energy for different subjects, here we aim to maximize the minimum of the average power across different subjects. That is, we choose m, k and D such that the minimum average power, across the subjects, is maximized.

Since the collision of the mass to the internal wall of the frame loses energy, and introduces non-linearities, the movement of the mass is kept limited to $|r(t)| \leq r_L$. In other words, the parameters m, k and D are considered to be *valid* if the movement of the internal mass satisfies the constrain $|r(t)| \leq r_L$ for all t and all subjects. This is similar to the approach used in [22].

The mass m and the size constrain r_L are usually given by the configuration of a VDRG system. We consider a medium-sized configuration for the VDRG acceleration-to-power generator, which can be manufactured using standard precision engineering technology [22]. The system parameters of the VDRG configuration are $m = 0.5$ g and $r_L = 1$ mm. To summarize, we optimize parameters k and D by maximizing the smallest average harvesting power of all subjects over the valid set of parameters. Or

$$\begin{aligned}(k^\star, D^\star) = \arg\max_{k,D} \min_{s} \quad & \bar{P}_s \\ \text{subject to} \quad & |r_s(t)| \leq r_L\end{aligned}$$

where s is the subject index and $\bar{P}_s$ is the average power for subject s.

3. MARKOVIAN MODEL

We divide each two day measurement into two one day segments. We fit the first day data to a Markovian model, and verify the goodness of fit by comparing the Markovian model with the second day data.

3.1 Optimal Quantization

The harvesting power $p(t)$ is quantized into a two-level harvesting power $p_b(t)$. The optimal threshold τ is obtained by using a non-uniform Lloyd-Max quantizer [15] which minimizes the mean-square quantization error between $p(t)$ and $p_b(t)$. After obtaining the optimal threshold, the binary harvesting power is

$$p_b(t) = \begin{cases} p_M & p(t) > \tau \\ p_m & p(t) < \tau \end{cases},$$

where

$$\begin{aligned} p_M &= \frac{\int_{p(t)>\tau} p(t)dt}{\int_{p(t)>\tau} dt} \\ p_m &= \frac{\int_{p(t)<\tau} p(t)dt}{\int_{p(t)<\tau} dt}. \end{aligned}$$

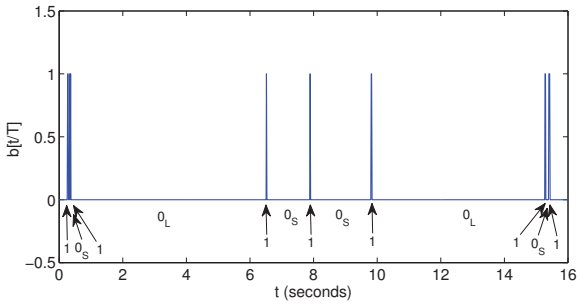

Figure 3: An example of a piece of $b[n]$ and $s[n]$

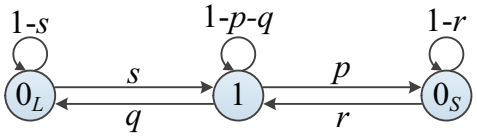

Figure 4: Markov chain of modeling the binary signal $b(t)$

3.2 Markovian Model

In order to model the harvesting power by a discrete-time Markov chain, the two-level harvesting power $p_b(t)$ is converted into a binary signal $b[n]$, where $b[n] = 0$ if $p_b(nT) = p_m$ and $b[n] = 1$ otherwise. Note that the acceleration data is recorded with a sampling frequency 75 Hz, thus $T = 1/75$ s. Fig. 3 shows an example of a section of the binary signal $b[n]$. Inspection of the binary signal $b[n]$, reveals that consecutive repetitions of 0s (runs of 0s) can clearly be divided into two distinct sets, one containing long runs of 0s and the other containing short runs of 0s, between two adjacent runs of 1. Therefore, we define the states 0_L and 0_S for the long and the short runs of 0s, respectively, as well as the state 1 for the runs of 1s. The three states, i.e. 0_L, 0_S, and 1, form a Markov chain as shown in Fig. 4. The transition probability matrix of the Markov chain is

$$\mathbf{P} = \begin{bmatrix} 1-s & q & 0 \\ s & 1-p-q & r \\ 0 & p & 1-r \end{bmatrix},$$

where $s \leq r$.

Let us denote the ith run of 0s followed by a run of 1s as follow

$$1 \to 0_0 \to 0_1 \to \cdots \to 0_{n_i} \to 1_0 \to 1_1 \to \cdots \to 1_{m_i} \to 0$$

where $n_i, m_i \geq 0$. The probability of such a cycle occurring is

$$\begin{aligned} Pr(n_i, m_i|0_L) &= (1-s)^{n_i} s(1-p-q)^{m_i}(p+q) \\ Pr(n_i, m_i|0_S) &= (1-r)^{n_i} r(1-p-q)^{m_i}(p+q). \end{aligned}$$

Thus,

$$\begin{aligned} Pr(n_i, m_i) &= q(1-s)^{n_i} s(1-p-q)^{m_i}(p+q) \\ &\quad +p(1-r)^{n_i} r(1-p-q)^{m_i}(p+q) \\ &= [q(1-s)^{n_i} s + p(1-r)^{n_i} r] \\ &\quad \times(1-p-q)^{m_i}(p+q). \end{aligned}$$

Assume that the whole binary signal $b[n]$ contains K cycles of 0s and 1s. Thus, the likelihood that $b[n]$ is an outcome of this Markov chain becomes $\prod_{i=1}^{K} Pr(n_i, m_i)$ and the log-likelihood of $b[n]$ is

$$\begin{aligned}\mathcal{L} &= \ln \prod_{i=1}^{K} Pr(n_i, m_i) \\ &= \sum_{i=1}^{K} \ln Pr(n_i, m_i) \\ &= \sum_{i=1}^{K} \ln[q(1-s)^{n_i} s + p(1-r)^{n_i} r] \\ &\quad + K\bar{m} \ln(1-p-q) + K \ln(p+q)\end{aligned}$$

where $\bar{m} = \frac{1}{K}\sum_{i=1}^{K} m_i$, is the average run length for 1s.

We therefore design our Markovian model by maximizing the log-likelihood of the first day data, $\mathcal{L}_1$

$$\begin{aligned}\underset{s,r,p,q}{\text{maximize}} \quad & \mathcal{L}_1 \\ \text{subject to} \quad & 0 \le s \le r \le 1 \\ & 0 \le p, q \\ & p + q \le 1.\end{aligned} \tag{2}$$

The optimized transition parameters are denoted by $s^\star$, $r^\star$, $p^\star$, $q^\star$, and the resulting maximum of log-likelihood is denoted by $\mathcal{L}_1^\star$. Using this approach, we fit the first-day empirical data of harvesting power to Markovian models for all subjects.

To evaluate the performance of the fitted Markovian model, we use the fitted parameters $s^\star$, $r^\star$, $p^\star$, $q^\star$ to calculate the log-likelihood $\mathcal{L}_2^\star$ of the second day empirical data for all subjects. Furthermore, the optimal log-likelihood $\mathcal{L}_2^\dagger$ is obtained by implementing the optimization problem (2) for the second day empirical data. We compare $\mathcal{L}_2^\star$ and $\mathcal{L}_2^\dagger$ by calculating

$$\Delta = \frac{\mathcal{L}_2^\dagger - \mathcal{L}_2^\star}{\left|\mathcal{L}_2^\dagger\right|}.$$

4. RESULTS

4.1 Harvested Energy

Using the VDRG configuration parameters $m = 0.5$ g and $r_L = 1$ mm, we optimize the system parameters k and D for the four body locations (ankle, left wrist, right wrist, and waist) and the three orthogonal directions, x-axis, y-axis, z-axis. For each scenario, we use the adaptive simulated annealing [8] to maximize the minimum average harvesting power $\bar{P}_{min}$ of all subjects. The resulting optimized parameters $k^\star$ and $D^\star$ and the resulting $\bar{P}_{min}$ are presented in Table 1.

In general, a vibration harvesting device is only able to harvest the energy along one direction [24]. By comparing $\bar{P}_{min}$ over the three directions for each location, it is clear that the maximum of $\bar{P}_{min}$ occurs along the y-axis for all locations. Therefore, we focus on the Markovian modeling of the harvesting power measured along the y-axis for all four locations.

Table 1: Optimized parameters of the VDRG harvester and the resulting minimum average harvested power.

Location	Axis	k (N/m)	D (Ns/m)	$\bar{P}_{min}$ (μW)
Ankle	x	7.302	1.140	0.328
	y	15.90	0.360	0.627
	z	16.63	0.193	0.167
Left Wrist	x	5.366	2.120	0.079
	y	6.168	2.355	0.106
	z^*	16.86	0.976	0.078
Right Wrist	x	3.121	2.204	0.097
	y	13.75	0.878	0.153
	z	7.159	2.141	0.067
Waist	x	6.546	0.659	0.074
	y	7.417	0.659	0.099
	z	14.21	0.266	0.031

*For the left wrist along the z-axis, the system parameters $k^\star$ and $D^\star$ are optimized without subject 11. This is due to the fact that, because of irregularities in this data set, its inclusion results in the impractical value of $k^\star = 4.848 \times 10^{-12}$.

4.2 Markovian Model

Fig. 5 depicts the histograms of p_m and p_M for each particular location. Moreover, the quantized harvesting power is fitted into a Markovian model with the optimized parameters $s^\star$, $r^\star$, $p^\star$, $q^\star$. For each particular location, the histograms of these optimized transition probabilities are plotted in Fig. 6. Since there are only 20 subjects we do not have the statistical significance to fit a probability distribution to these histograms. Therefore, the optimal quantization parameters and the optimized transition probabilities are presented by their means and standard deviations denoted by μ_{p_m}, μ_{p_M}, $\mu_{s^\star}$, $\mu_{r^\star}$, $\mu_{p^\star}$, $\mu_{q^\star}$, and σ_{p_m}, σ_{p_M}, $\sigma_{s^\star}$, $\sigma_{r^\star}$, $\sigma_{p^\star}$, $\sigma_{q^\star}$, respectively. Among all measurements for the ankle, we observe one outlier, subject 13, whose transition probabilities are significantly beyond the range of other subjects, as marked in Fig. 6(a). This outlier is removed from the calculation of mean and variance for the ankle location. The mean and the standard deviation of the quantization parameters and the fitted parameters are calculated and shown in Table 2. The table also provides $\bar{\Delta}$, which is Δ averaged over all subjects, as a goodness-of-fit measure.

To use the model, we suggests that the mean values $\mu_{s^\star}$, $\mu_{r^\star}$, $\mu_{p^\star}$, $\mu_{q^\star}$ are used as the transition probabilities of the Markovian source, and the mean values μ_{p_m} and μ_{p_M} as the harvesting powers associated with each state. In cases where it is desired to capture the variation from subject to subject, we suggest that the parameters are drawn from uniform distributions with given means and variances. Furthermore, since p_m is considerably smaller than p_M, it may be approximated with zero to yield an *on-off* model, where power p_M is harvested in the *on* state and no power is harvested in the *off* state.

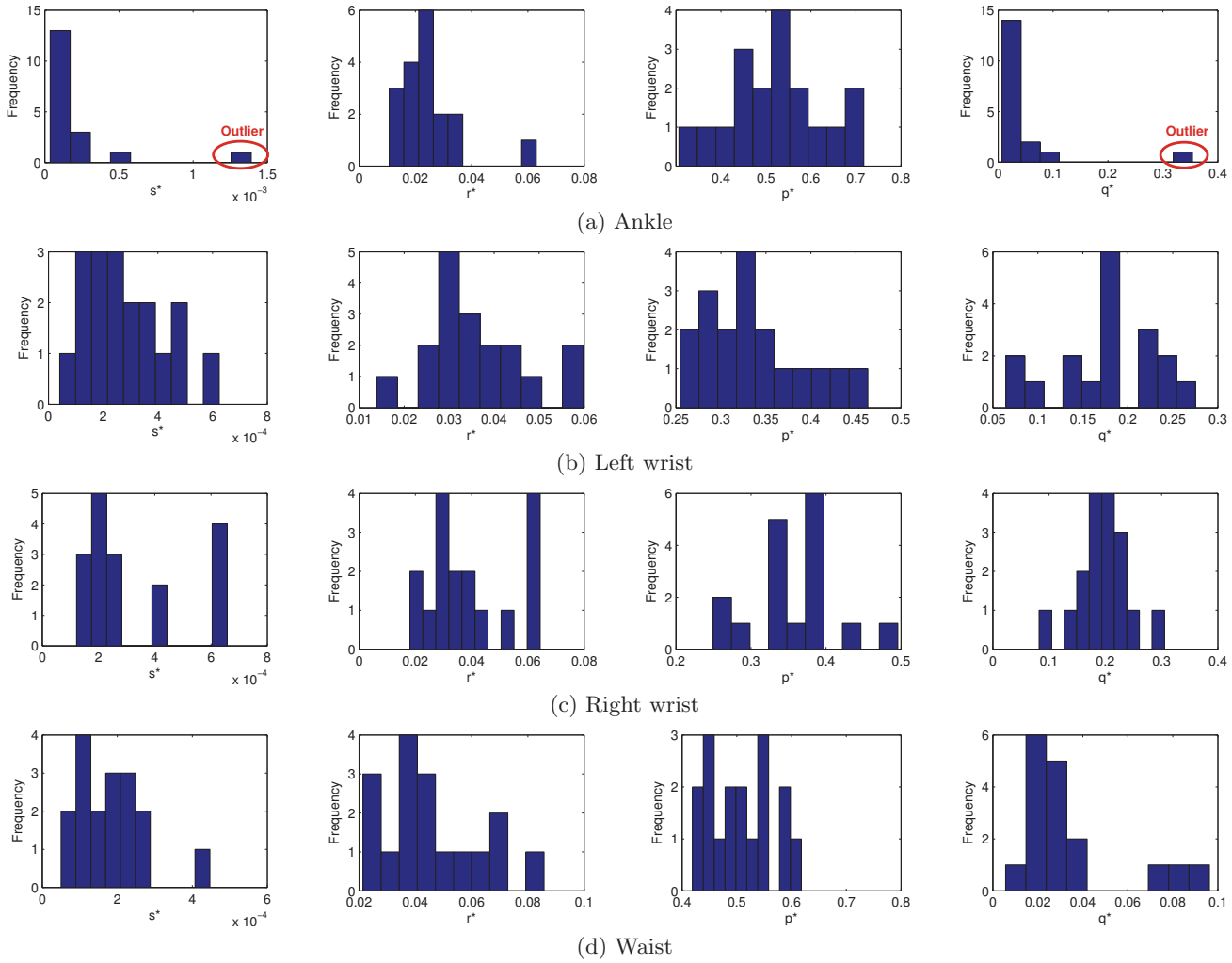

Figure 6: Histograms of the optimized parameters $s^\star$, $r^\star$, $p^\star$, $q^\star$.

5. CONCLUSION

In this paper, for the first time, we have provided a Markovian model for harvested power from human motion. The model is developed based on empirical measurements of acceleration at 4 body locations from 20 subjects, which is then converted to power assuming a VDRG harvester. The simple model provided consists of a "high-power" or "on" states and two "low-power" or "off" states (with different average dwelling times). While this simple model may not capture some details of the characteristics of the source dynamics, it provides a suitable tool for simulations and analysis.

6. REFERENCES

[1] C. Alippi and C. Galperti. An adaptive system for optimal solar energy harvesting in wireless sensor network nodes. *IEEE Transactions on Circuits and Systems*, 55(6):1742–1750, July 2008.

[2] Alive Technologies Pty Ltd. *Alive heart monitor: Bluetooth ECG and activity monitor.*

[3] P. Bonato. Advances in wearable technology and applications in physical medicine and rehabilitation. *Journal of NeuroEngineering and Rehabilitation*, 2(1):2, Feb. 2005.

[4] A. E. Şuşu, A. Acquaviva, D. Atienza, and G. De Micheli. Stochastic modeling and analysis for environmentally powered wireless sensor nodes. In *Proceedings of the 6th International Symposium on Modeling and Optimization in Mobile, Ad Hoc, and Wireless Networks and Workshops (WiOpt)*, pages 125–134, Apr. 2008.

[5] K.-W. Fan, Z. Zheng, and P. Sinha. Steady and fair rate allocation for rechargeable sensors in perpetual sensor networks. In *Proceedings of the 6th ACM conference on Embedded network sensor systems (SenSys)*, pages 239–252, Nov. 2008.

[6] C. K. Ho, P. D. Khoa, and P. C. Ming. Markovian models for harvested energy in wireless communications. In *Proceedings of 2010 IEEE International Conference on Communication Systems (ICCS)*, pages 311–315, Nov. 2010.

[7] J. Hsu, S. Zahedi, A. Kansal, M. B. Srivastava, and V. Raghunathan. Adaptive Duty Cycling for Energy Harvesting Systems. In *Proceedings of the 2006 International Symposium on Low Power Electronics*

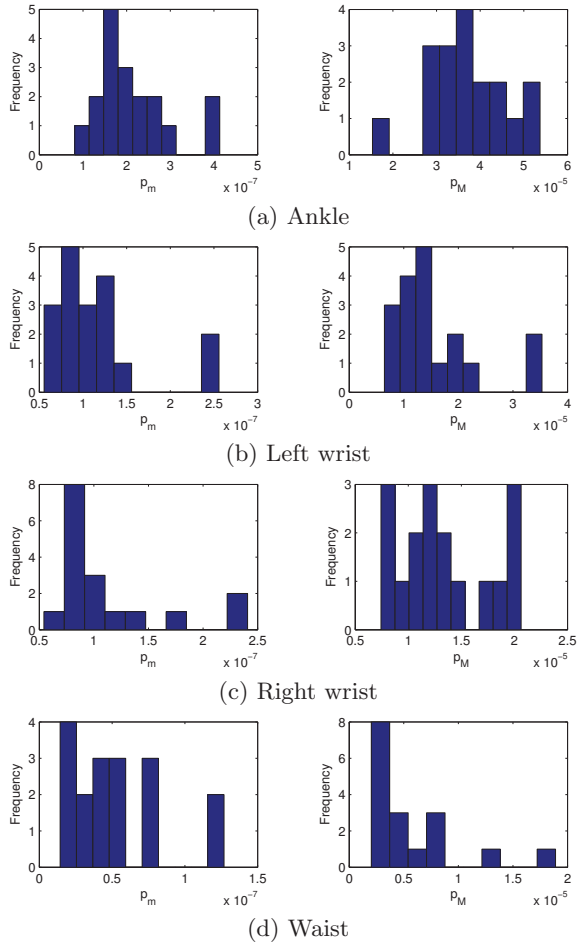

(a) Ankle

(b) Left wrist

(c) Right wrist

(d) Waist

Figure 5: Histograms of the optimal quantization parameters p_m and p_M.

Table 2: The fitted parameters of Markovian models and the resulting performance.

Par.	Ankle**	Left wrist	Right wrist	Waist
μ_{p_m} (μW)	2.1×10^{-1}	1.2×10^{-1}	1.1×10^{-1}	5.2×10^{-2}
σ_{p_m} (μW)	8.8×10^{-2}	5.2×10^{-2}	5.3×10^{-2}	3.1×10^{-2}
μ_{p_M} (μW)	3.7×10^{1}	1.6×10^{1}	1.4×10^{1}	5.8
σ_{p_M} (μW)	9.4	7.8	4.3	4.3
$\mu_{s^\star}$	1.5×10^{-4}	2.9×10^{-4}	3.2×10^{-4}	1.8×10^{-4}
$\sigma_{s^\star}$	1.0×10^{-4}	1.5×10^{-4}	1.9×10^{-4}	9.6×10^{-5}
$\mu_{r^\star}$	2.2×10^{-2}	3.6×10^{-2}	3.9×10^{-2}	4.5×10^{-2}
$\sigma_{r^\star}$	6.4×10^{-3}	1.1×10^{-2}	1.5×10^{-2}	1.8×10^{-2}
$\mu_{p^\star}$	5.4×10^{-1}	3.4×10^{-1}	3.6×10^{-1}	5.1×10^{-1}
$\sigma_{p^\star}$	9.1×10^{-2}	5.6×10^{-2}	5.7×10^{-2}	5.8×10^{-2}
$\mu_{q^\star}$	3.1×10^{-2}	1.8×10^{-1}	2.0×10^{-1}	3.4×10^{-2}
$\sigma_{q^\star}$	1.6×10^{-2}	5.6×10^{-2}	4.9×10^{-2}	2.4×10^{-2}
$\bar{\Delta}$	1.8×10^{-2}	1.7×10^{-2}	1.3×10^{-2}	1.0×10^{-2}

**For the ankle location, the outlier subject 13 is removed from the calculation of the mean and the standard deviation of the fitted parameters.

and Design (ISLPED), pages 180–185. IEEE, Oct. 2006.

[8] L. Ingber. Simulated annealing: Practice versus theory. *Mathematical and Computer Modelling*, 18(11):29–57, Dec. 1993.

[9] X. Jiang, J. Polastre, and D. Culler. Perpetual environmentally powered sensor networks. In *Proceedings of the 4th International Symposium on Information Processing in Sensor Networks (IPSN)*, pages 463–468, Apr. 2005.

[10] E. Jovanov, A. Milenkovic, C. Otto, and P. C. de Groen. A wireless body area network of intelligent motion sensors for computer assisted physical rehabilitation. *Journal of Neuroengineering and Rehabilitation*, 2(1):6, Mar. 2005.

[11] H. Karl and A. Willig. *Protocols and Architectures for Wireless Sensor Networks*. John Wiley & Sons, 2005.

[12] J. W. Kimball, B. T. Kuhn, and R. S. Balog. A system design approach for unattended solar energy harvesting supply. *IEEE Transactions on Power Electronics*, 24(4):952–962, Apr. 2009.

[13] J. Lei, R. Yates, and L. Greenstein. A generic model for optimizing single-hop transmission policy of replenishable sensors. *IEEE Transactions on Wireless Communications*, 8(2):547–551, Feb. 2009.

[14] V. Leonov, T. Torfs, P. Fiorini, and C. V. Hoof. Thermoelectric converters of human warmth for self-powered wireless sensor nodes. *IEEE Sensors Journal*, 7(5):650–657, May 2007.

[15] J. Max. Quantizing for minimum distortion. *IRE Transactions on Information Theory*, 6(1):7–12, Mar. 1960.

[16] P. D. Mitcheson, T. C. Green, E. M. Yeatman, and A. S. Holmes. Architectures for vibration-driven micropower generators. *Journal of Microelectromechanical Systems*, 13(3):429–440, June 2004.

[17] S. Patel, K. Lorincz, R. Hughes, N. Huggins, J. Growdon, D. Standaert, M. Akay, J. Dy, M. Welsh, and P. Bonato. Monitoring motor fluctuations in patients with ParkinsonâĂŹs disease using wearable sensors. *IEEE Transactions on Information Technology in Biomedicine*, 13(6):864–873, Nov. 2009.

[18] W. K. G. Seah, Z. A. Eu, and H.-P. Tan. Wireless sensor networks powered by ambient energy harvesting (WSN-HEAP) - survey and challenges. In *Proceedings of the 1st International Conference on Wireless Communication, Vehicular Technology, Information Theory and Aerospace and Electronic Systems Technology (Wireless VITAE)*, pages 1–5, May 2009.

[19] A. Seyedi and B. Sikdar. Modeling and analysis of energy harvesting nodes in wireless sensor networks. In *Proceedings of the 46th Annual Allerton Conference on Communication, Control, and Computing*, pages 67–71, Sept. 2008.

[20] Y. K. Tan and S. K. Panda. Optimized wind energy harvesting system using resistance emulator and active rectifier for wireless sensor nodes. *IEEE Transactions*

on Power Electronics, 26(1):38–50, Jan. 2011.

[21] C. M. Vigorito, D. Ganesan, and A. G. Barto. Adaptive control of duty cycling in energy-harvesting wireless sensor networks. In *Proceedings of the 4th Annual IEEE Communications Society Conference on Sensor, Mesh and Ad Hoc Communications and Networks (SECON)*, pages 21–30, June 2007.

[22] T. von Büren, P. D. Mitcheson, T. C. Green, E. M. Yeatman, A. S. Holmes, and G. Tröster. Optimization of inertial micropower generators for human walking motion. *IEEE Sensors Journal*, 6(1):28–38, Feb. 2006.

[23] T. von Büren and G. Tröster. Design and optimization of a linear vibration-driven electromagnetic micro-power generator. *Sensors and Actuators A: Physical*, 135(2):765–775, Apr. 2007.

[24] G.-Z. Yang, editor. *Body Sensor Networks*. Springer, 2006.

[25] S. Zhang, A. Seyedi, and B. Sikdar. An Analytical Approach to the Design of Energy Harvesting Wireless Sensor Nodes. *to appear in IEEE Transactions on Wireless Communications*, 2013.